Laser Multi-layer Cladding Experiment on the DD3 Single Crystal Using FGH95 Powder: Investigation on the Microstructure of Single Crystal Cladding Layer

FENG Li-ping, HUANG Wei-dong, LIN Xin, YANG Hai-ou, LI Yan-min, Yang Jian
(*State Key Laboratory of Solidification Processing, Northwestern Polytechnical University, Xi'an 710072, China*)

Abstract: Lasermulti-layer cladding experiments were performed on the substrate of DD3 single crystal with FGH95 powder as cladding material. The solidification microstructure in the sample was investigated. It was found that the solidification microstructure was greatly influenced by the crystallography orientation of the substrate and the local solidification conditions. When the angle between the preferred orientation of the single crystal and the direction of heat flow in the cladding layer is less than 30°, single crystal cladding layers were acquired. Otherwise the crystallography orientation of the cladding layer will deviate from the orientation of the substrate and the microstructure with polycrystalline appears. Meanwhile, even when the experiments were performed on the same preferred crystal surface, the solidification microstructures will be different distinctly resulting from the variation of the local solidification conditions. The secondary arms were degenerated and the primary arm spacing was about 10–20 μm. Further investigation shows that the phases of the cladding layer are mainly made up of γ, γ′, the flower-like γ/γ′ eutectic and carbide. The morphology of γ′ was cubical and the size is less than 0.1μm.

Key words: laser metal forming directional solidification; laser multi-layer cladding; single crystal; microstructure; composition segregation

在 **DD3** 单晶上进行 **FGH95** 粉末激光多层涂覆: 单晶涂层组织形式规律研究 . 冯莉萍, 黄卫东, 林鑫, 杨海鸥, 李延民, 杨健 . 中国航空学报(英文版), 2002, 15(2): 121- 127.

摘 要: 利用高温合金 FGH95 粉末在 DD3 单晶的不同晶面上进行激光多层涂覆实验, 深入研究了涂覆层中凝固显微组织的生长规律。研究表明基材的晶体取向和局部凝固条件对涂层中的凝固显微组织有很大的影响。当单晶基材择优晶向与热流方向夹角小于 30 时, 可以得到从基材上外延生长的单晶, 涂层内二次臂退化, 枝晶一次间距为 10～20μm; 当实验所在的单晶基材的择优晶向与热流的方向夹角大于 30 时, 涂层中晶体取向偏离基材的取向, 并出现多晶。即便当实验在同一个择优晶面上进行时, 局部凝固条件不同, 涂层内的凝固显微组织也有很大的差别。二次臂退化, 一次臂间距大约为 10～20μm。进一步的研究表明, 涂层中主要组成相为枝晶干上分布的基体相 γ 和沉淀硬化相 γ′ 以及枝晶间的 γ+ γ′ 花状共晶和少量碳化物, γ′ 相主要为具有良好强化效果的细小立方体, 尺度约为 0.1μm。

关键词: 激光金属成形定向凝固; 激光多层涂覆; 单晶; 显微组织; 成分偏析
文章编号: 1000-9361(2002)02-0121-07 中图分类号: V252; TG132 文献标识码: A

During directional solidification, increasing the liquid temperature gradient in front of the solid/liquid interface can refine the solidification microstructures and thus improve the comprehensive properties of superalloys. Researchers in the directional solidification field have been pursuing higher liquid temperature gradient in front of the solid/liquid interface for many years. At present, the

Received date: 2001-11-20; Revision received date: 2002-04-02
Foundation item: National Key Basic Research Development Programme of china (No. G2000067205-3)
Article URL: http://www.hkxb.net.cn/cja/2002/02/0121/

temperature gradient of about 1300K/cm can be obtained by means of combining the zone melting and liquid metal cooling. Under such a high temperature gradient, the superfine directional solidification columnar microstructure was obtained, which makes the properties of nickel-base superalloys improved clearly in comparison with those of the conventional directional solidification[1].

With the development of laser processing, much higher temperature gradient ($10^5 \sim 10^7$K/m) can be obtained in the melting pool than that mentioned above. So it is possible to create a new directional solidification technique with ultrahigh temperature gradient with laser as a heat source. Thin film with directional solidification microstructure was obtained through laser remelting[2-4]. In order to realize the manufacture of bulk directional solidification samples with ultrahigh temperature gradient, it is instructive to develop a novel laser directional solidification technique.

Laser metal forming[5, 6], a new near net shaping technique developed recently, which combined rapid prototyping with multi-layer cladding with ultrahigh temperature gradient, can meet this need. The solidification microstructure in the melting pool grew epitaxially from the substrate during laser cladding. If the single crystal was selected as a substrate, the sample with thin directional solidification columnar dendrites or even single crystal can be obtained.

In this paper, the multi-layer cladding experiments were performed on the top, the cylinder surface and the circle of the cylindrical DD3 single crystal rod by a careful selection of the processing parameters. The forming law of single crystal cladding layers on the different crystallography planes was summarized and the theory of manufacturing single crystals with laser multi-layer cladding was established. The ultimate aim of this paper is to explore a novel path to acquire single crystal samples with complex shapes.

1 Experimental Procedure

Experiments were performed with a 5 kW continuous wave CO_2 laser. The beam diameter is 5mm. The powder deposit system consists of a scraper powder feeder and a lateral-cladding nozzle with a laminar flow of protective gas (Ar). Processing parameters were as follows: laser power 3-4kW, solidification velocity 5-10mm/s, powder feeding 7-12g/min and protective gas flux 5-10ml/min, respectively.

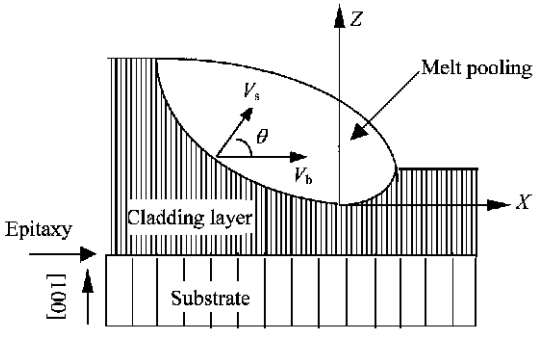

Fig. 1 Schematic diagram of the epitaxial columnar dendritic growth in the laser melting pool

DD3 single crystal rod with the diameter of about 15mm was selected as the substrate. The crystallographic orientation of the top surface is 〈001〉. Since there is no commercial powder of DD3 single crystal superalloy, the FGH95 used for HIP (hot isotropic pressure) aeronautical turbine disk was used, because the composition of FGH95 alloy is similar to that of the DD3 single crystal. The chemical composition of the FGH95 powder and the DD3 substrate is shown in Table 1. The size of the powder is less than 200 meshes. The angle between the axial of the cylindrical single crystal rod and the preferential crystallography of the dendrite in the rod is about 10°. To analyze the effect of different crystallography planes on the solidification morphology in the layer, three different cladding directions are taken (Fig. 2). In Fig. 2, Schemes 1 and 2 are focused on investigating the solidification microstructure in the cladding layers when the experiment is performed on the preferential crystallography planes, and the aim of Scheme 3 is to study the variation of the solidification microstructure with the angle between the preferred orientation of the single crystal and the direction of heat flux. Microstructure observation was carried

out with optical microscope (OM) and scanning electron microscope (SEM).

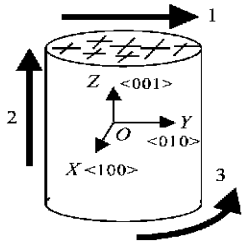

ig. 2 Experimental scheme of laser multi-layer cladding

Table 1 Nominal composition of the substrate and powder(wt%)

Material	C	Cr	Co	Al	Ti	Mo
FGH95	0.07	13	8	3.5	2.6	3.5
DD3	0.06	9.5	5	5.7	2.3	4.2
Material	W	Nb	Zr	B	Ni	
FGH95	3.5	3.8	0.05	0.010	Bal.	
DD3	5.2	–	< 0.005	Trace	Bal.	

2 Results and Discussions

2.1 Microstructure

Fig. 3 (a) shows the solidification microstructure of the interface between the cladding layer and the substrate, which was acquired on the top of the single crystal rod. From Fig3 (a), it can be found that the solidification microstructure in the cladding layer is much thinner than that of the substrate apparently. The interface between the substrate and the cladding layer is ripple. It is due to the composition segregation between the dendrite trunk and the interdendritic areas in the substrate. The white part in the substrate is the trunk of the dendrites where the negative segregation element, such as Co, W, were segregated, and this part melted finally, while some of the elements, such as Al, Ti, Cr, which are easy to form the low melting point eutectic, were accumulated in the interdendritic areas, and these areas will melt at first (The EDS results of the points "1" and "2" shown in Fig. 3 (a) are listed in Table 2), and thus causing the unevenness of the interface. From Fig. 3 (a), one can also find that there exist several micro-zones with the horizontal growth microstructure just on the concave part of the interface. The forming of these zones is resulting from the horizontal solution distribution, *i.e.* solute concentration on the convex is higher than that of the concave of the interface, so the dendrites will grow along the composition gradient preferentially. Fig. 3 (b) shows the solidification

Table 2 EDS results of different places in the substrate(wt%)

Different places	Al	Ti	Cr	Co	Ni	Mo	W
1	5.46	0.94	9.05	5.59	68.16	3.66	7.15
2	5.55	2.85	10.98	4.98	66.02	6.49	3.12

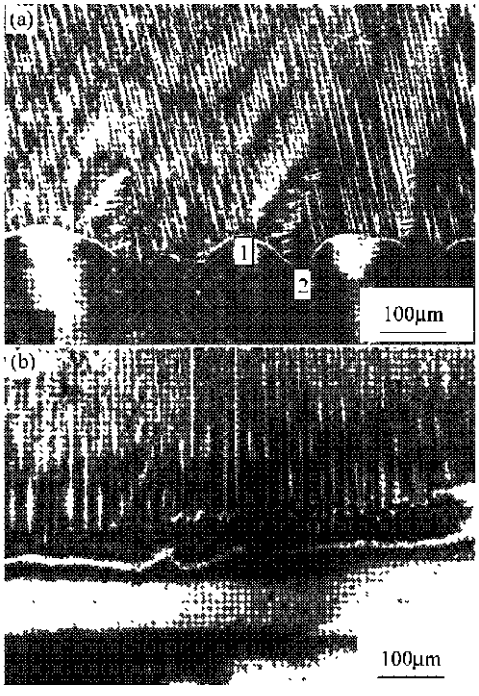

Fig. 3 Microstructure of the transverse section of interface of the sample under different experiment conditions
(a) Microstructure on the top of the columnar single crystal;
(b) Microstructure on the side of the columnar single crystal

microstructure of the transverse section at the interface when the cladding is along the cylinder of the single crystal rod. The solidification microstructure in the layer grows up normal to the interface. The growth direction is just the direction of the secondary trunk of the columnar dendritic in the substrate. It is known that under the condition of the positive temperature gradient, dendrite trunks, whose crystal orientations are closest to the heat flux, will grow preferentially due to the anisotropy of the interface energy and the growth

kinetics. Since the crystal structure of nickel-base superalloy is face center cubical (fcc), both the trunk and the side branch grow along the [001] crystallography orientation[7] and the secondary trunk direction is another preferential crystallography direction (⟨010⟩). Successful single crystals can be obtained when the experiment was performed on this plane.

From Fig. 3, it can also be seen that, in the cladding layers, the primary arm spacing is small, and the secondary arm tends to degenerate. It is due to the fact that laser cladding is a processing with high growth velocity and high temperature gradient, the cooling rate under this experiment condition is about 10^3K/s, and there are no enough space and time for the secondary arm to grow up.

Fig. 4 to Fig. 7 exhibit microstructure photographs of the sample with the cladding along the circular of the DD3 single crystal rod. From Fig. 4, one can find the regular "+" pattern emerges in the middle part of the single crystal rod after macro-corrosion. This pattern is the typical

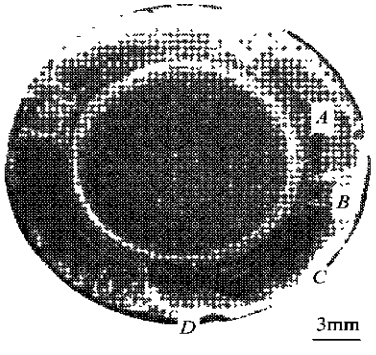

Fig. 4 Macrostructure of the transverse section of the sample (experiments were performed along the circular of the single crystal)

foundry single crystal structure. In the initial part of the circular cladding layers, a whole thinner dendrite layer grows epitaxially from the substrate. With increasing of the cladding layers, the apparently different growth morphologies are as follows: in the area where the angle between the heat flux and the preferential crystallography orientation is small, the clad layers push ahead with the same crystallography orientation as the substrate, while in the area in which the angle between the heat flux and the preferential crystallography orientation is large, there emerges multi-grain microstructure. The more the cladding layers, the more the grains appear. The region with multi-grain microstructure is like an opening fan, the central angle of which is about 30°. That is to say, when the angle between the preferential crystallography and the direction of the heat flux is less than 30°, the single crystal clad layers that grow epitaxially from the substrate can be obtained. These regions can be clearly seen in Fig. 4 marked with "*A*", "*B*", "*C*" and "*D*" based on the above description. In region *A*, epitaxial growth dendrite with the orientation identical to the substrate is presented. While region *B* is characterized by a layer of the epitaxial single crystal dendrite zone along the orientation of the secondary trunk that has 45° deviation with the horizontal interface, while in the middle part of region *B*, there exists multi-grain microstructure deviated from the former crystallography orientation, which indicates that heterogeneous nucleation appears in the melting pool. In the whole outer circular cladding layers, there exist random orientation dendrite layers (region *C*) and a special zone (region *D*); in region *D* the initial part of the cladding layer is the same as that of zone *A*, while on the top of the cladding layers, the crystallography orientation deviated 90° to the original orientation grows previously.

Fig. 5 exhibits microstructure photography of region *A* in Fig. 4. From Fig. 5, it can be found that the solidification microstructure is thin and dense; the spacing of the dendrites is about 10–20μm. Since the direction of this secondary arm is also a preferential orientation, the epitaxial growth directional dendrites can be obtained. The microstructure with white and bright dot is due to the fact that the section displayed does not cross the trunk of the dendrite appropriately but has about 10° deviations. For this alloy, when experiments were performed on any preferential planes, the single crystal cladding layer with fine orientation can be obtained easily under the suitable processing parameters.

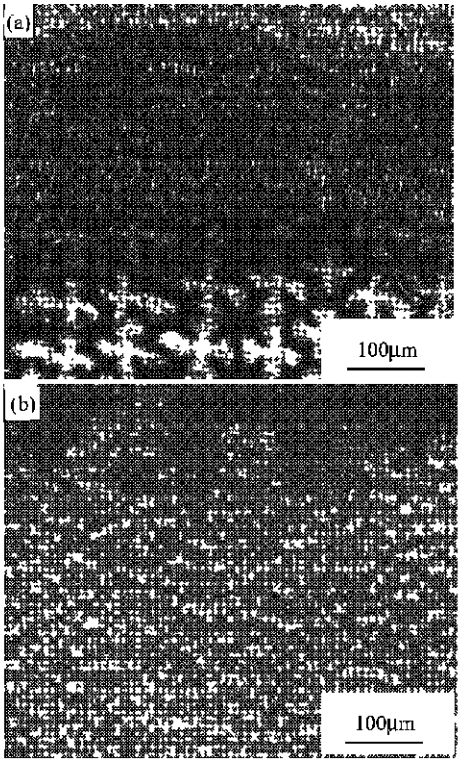

Fig. 5 Microstructure of cross section of the region *A*
a) at the interface; (b) in the inner part and the surface

Fig. 6 is the solidification microstructure of region *B* in Fig. 4. Evidently different from that of the region *A*, when experiments were performed on the non-preferential crystallography plane, there first appears a thin layer of epitaxial growth thin dendrites. The crystallography orientation in this cladding layer is the same as that of the substrate. While in the middle part of the cladding layers, the crystallography orientation that deviated about 45 °from the heat flux will lose the growing superiority and there appear columnar grains with different crystallography orientations. The crystallography orientation of these grains has no fixed orientation relationship with that of the substrate. This shows that there exists columnar equiaxed transition (CET) in front of the solid/liquid interface of the melting pool. According to the solidification theory, when there are enough nucleuses in the supercooling zone in front of the solid/liquid interface, the growth of the columnar will be restrained and novel columnar deviated from the original columnar or even equiaxed grains appeared[8]. Under the processing condition mentioned in this paper, when the experiment was performed on different crystallography orientation planes, the supercooling of the dendrite tip is different due to the different angles between the directions of the dendrite growth and the temperature gradient. When the angle between the preferential orientation and the direction of the heat flow is large, for the same interface pushing velocity, the growth velocity of the dendrites is larger than that with the small angle between the preferential crystallography orientation and the direction of heat flux. Thus the undercooling of the dendrites tip is larger, and the conditional undercooling zone will be wide too, which makes the nucleation become easier and transition of the columnar to the equiaxed appear. This is the possible reason why there exists epitaxial growth in region *A* while there appears new crystal in region *B*. So to avoid nucleation and CET in front of the solid/liquid interface is no doubt a prerequisite to acquire the single crystal cladding layer successfully. As FGH95 is a multi-component nickel-base superalloy and

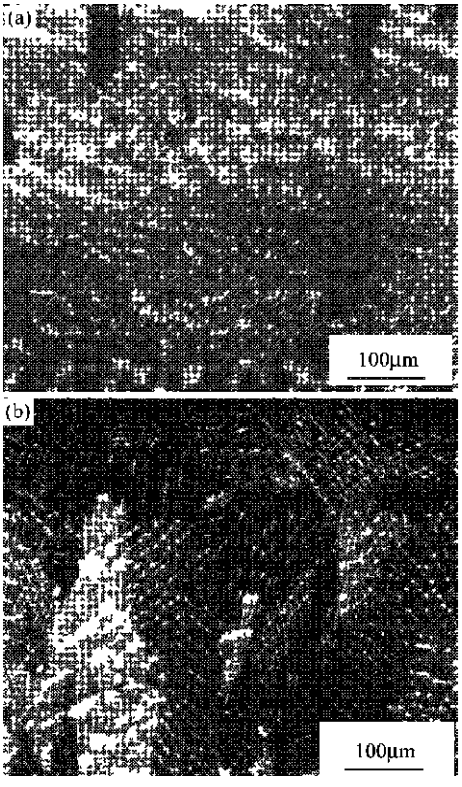

Fig. 6 Microstructure of the cross section of the region *B*
(a) in interface; (b) in the inner part and the surface

there are no thermodynamic parameters in publicity, it is hard to calculate the CET accurately, and one can only explain the phenomena described above qualitatively according to the solidification theory.

Fig. 7 is the solidification microstructure photography of the region *D* in Fig. 4. From Fig. 7 (a), one can find that the thin columnar dendrites grow epitaxially from one of the preferential crystallography of the substrate. Fig. 7 (b) shows the microstructure of the outside of the cladding layers. The difference with Fig. 6 is that the direction changed dendrite has fixed orientation relationship with the main growth direction. In the whole direction changed zone, the crystallography orientation is identical to the orientation of the secondary arm, which is also a preferential crystallography orientation. This can be explained that there is no nucleation in this zone. This new growth morphology is due to a tilting of the primary growth direction by 90 °due to a change in the shape of the isotherms, which results in the dendrite branches of the columnar dendrites to become dendrite trunks. Analyzing the solidification condition of this region, one can presume that it is the zone where the cladding experiment is over. The modification of temperature gradient leads to abrupt (90 °) changes of the growth direction when the undercooling of the dendritite trunk tip is equal to the dendrite branch tip. The secondary arm, with another preferential crystallography orientation, will grow, and form the solidification microstructure shown in the photography. The top of the cladding layer can be remelted in the next deposit, thus the solid/liquid interface is moving ahead as a kind of sequential solidification. Under the constant processing condition, the latter deposits can grow up epitaxially on the former ones. As for the random dendrites region *C*, only presenting on the top of the last trace, can be removed by a final machining operation.

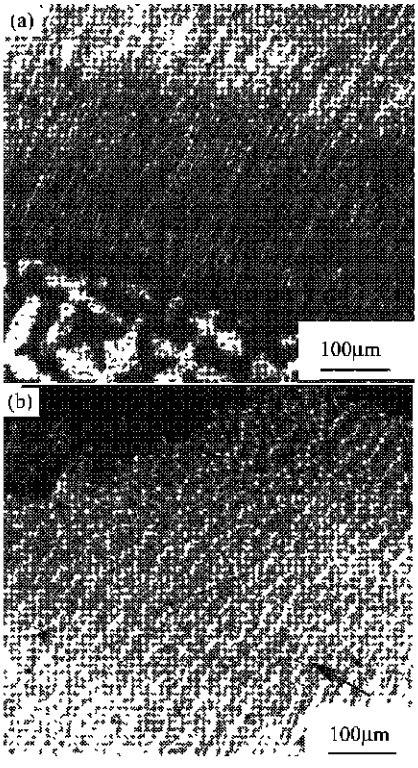

Fig. 7 Microstructure of the cross section of the region *D*
(a) in the interface; (b) in the inner part and the direction changed microstructure of the top of the layer

2.2 Phase morphology

Fig. 8 (a) is the TEM morphology of γ' particles distributed on the matrix. It is found that there exist different dimensions of γ' that are spherical and are smaller than 0.1μm due to the high cooling rate in the laser processing. The reason why there are different dimensions of γ' particle is that the local solidification conditions are different in different areas of the cladding layer. The area marked *A* in the figure is deduced to be dendritic trunk where the dimension of γ' is small, while the place where the size of γ' is large corresponds to the interdendrite area. So a suitable heat treatment scheme must be adopted to acquire homogeneous γ' particles.

Fig. 8 (b) shows the white flower-like eutectic and the black blocky γ' deposits arrayed parallel to the direction of the heat flux. Because there exists slight element segregation during rapid solidification, the residual liquid in the interdendrite areas is accumulated γ' particles forming elements such as Al, Ti, *etc*. When solidification happens, the composition of these residual liquids can form γ/γ' eutectic. The white blocky embraced in the eutec-

tic was phases rich in Nb, Mo and W. As these three elements are easy to form carbide, it can be induced that the white blocky is carbide(EDS results of different phases are shown in Table 3).

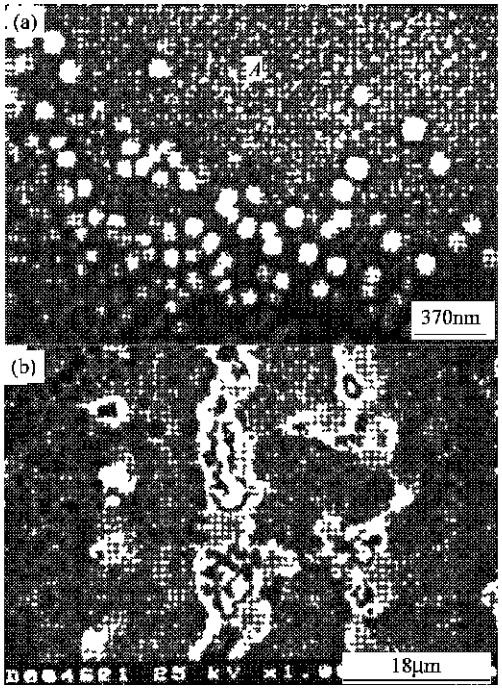

Fig. 8 Different phases in the cladding layers
(a) TEM morphology of γ' in different areas;
(b) Flowerlike (γ+ γ') eutectic in the substrate

Table 3 EDS result of different phases in the cladding layer(wt %)

Different phases	Al	W	Nb	Mo	Ti	Cr	Co	Ni
A	2.82	7.06	2.12	3.58	1.78	12.46	7.94	62.22
B	3.17	6.70	5.71	4.40	3.09	11.73	7.19	58.02
C	0.80	10.72	18.53	13.18	1.94	13.32	7.54	33.97

3 Conclusions

(1) When laser multi-layer cladding experiments were performed on the preferential crystallography planes of a single crystal, the single crystal cladding layer can be obtained. The columnar dendrites in the cladding layers are thin and dense. The primary arm spacing is around 10-20μm and the secondary side-branch is considerably degenerated.

(2) When laser multi-layer cladding experiments were performed on the non-preferential crystallography planes of the single crystal, the epitaxial growing columnar dendrites near the interface between the substrate and cladding layers can be obtained under the experiment conditions in this paper. While in the middle part of the cladding layers, the dendrite with this crystallography orientation loses growth superiority, which results in forming the random multi-grain cladding layers.

(3) The forming law of solidification microstructure in the cladding layer depends not only on the crystallography planes but also on the local solidification condition. Avoiding the transition of columnar to equiaxed in front of the solid/liquid interface is the prerequisite to acquire the single crystal cladding layer successfully.

(4) TEM and SEM analyses show that there are γ' deposits, γ/γ' flower-like eutectic and some carbide in the matrix. The morphology of the γ' particles is spherical, the size of which is less than 0.1μm.

References

[1] Li J G, Mao X M, Fu H Z. Interface morphologies and microstructures during dendrite-to-cell transition at high growth rate[J]. Acta Metall Sinica, 1991, 26(4): A309-312.
[2] Pan Q Y, Huang W D, *et al*. The solidification microsture and micro segregation behavior of a nickel-base superalloy under ultra-high temperature gradient conditions produced by a laser beam[J]. Journal of Materials Science Letters, 1996, 15: 2112- 2114.
[3] Cline H E. Growth of eutectic alloy thin films[J]. Mater Sci Eng, 1984: 65- 93.
[4] Cline H E. Interlamellar spacing in directionally solidified eutectic thin films[J]. Metall Trans, 1984, 15A: 1013- 1016.
[5] Gäumann G, Bezencon C, Canalis P, *et al*. Single-crystal lasers deposition of superal loys: processing-microstructure maps[J]. Acta Mater, 2001, 49: 1051- 1062.
[6] Gäumann M, Henry S, Cleton F, *et al*. Epitaxial laser metal forming: analysis of microstructure formation[J]. Mater Sci and Eng, 1999, A271: 232- 241.
[7] Kurz W, Fisher D J. Fundamentals of Solidification[M]. 4th ed Switzerland: Trans Tech Publication, 1984. 240.
[8] Hunt J D. Steady state columnar and equiaxed growth of dendrites and eutectic[J]. Mater Sci and Eng, 1984, 65: 75 - 83.

Biographies:

FENG Li-ping Born in 1973, Ph.D student, Email: fenglp0448@sina.com, Tell: 029-8494001.

HUANG Wei-dong Born in 1956, Ph. D, Professor, he is the director of State Key Loboratory of Solidification Processing of Northwestern Polytechnical University. Email: Huang @nwpu.edu.cn, Tel: 029-8494510.